International Research Journal of Engineering Science, Technology and Innovation (IRJESTI) Vol. 2(1) pp. 8-16, January, 2013
Available online http://www.interesjournals.org/IRJESTI

Full Length Research Paper

Effects of thermal radiation and magnetic field on heat transfer in a micropolar fluid along a vertical stretching surface with a variable viscosity and internal heat generation

N. T. Eldabe[1], E. M. A. Elbashbeshy[2] and E. M. Elsaid[3*]

[1]Department of Mathematics, Faculty of Education, Ain Shams University, Heliopolis, Cairo, Egypt
[2]Department of Mathematics, Faculty of Science, Ain Shams University, Abbassia, Cairo, Egypt
[*3]Department of Communications, Faculty of Engineering, Akhbar El Yom Academy, 6 October, Egypt

Accepted January 18, 2013

Effects of thermal radiation and magnetic field on heat transfer in a micropolar fluid along a vertical porous stretching surface in the presence of internal heat generation and variable viscosity are studied. The governing equations are transformed into a system of ordinary differential equations and solved them numerically using Mathematical program. The obtained results **are checked against previously published work for special cases of the problem in order to access the accuracy of the numerical method and found to be in excellent agreement Effects of the various parameters on the velocity profiles, temperature profiles and rate of heat transfer are also displayed graphically and tabulated form.**

Keywords: Thermal radiation, magnetic field, heat generation or absorption, stretching surface, micropolar fluid, variable viscosity.

INTRODUCTION

The boundary layer flow over a stretching surface have many practical applications in several engineering processes, for example, paper production, glass blowing, wire drawing and glass fiber production. Since the pioneering study by (Sakiadis, 1961 and 1961)who initialed the study of boundary layer flow over a continuous solid surface moving with constant speed. Crane (1970) extended the problem of Sakiadis (1961) who presented an exact analytical solution for the steady two dimensional stretching of surface in a quiescent fluid. The flow field of stretching surface with a power-law velocity variation was discussed by Banks (1983), Ali (1995) and Elbashbeshy (1998) extended the work of Banks (1983) for a porous stretched surface with different values of the injection parameter. Elbashbeshy and Bazid (2000, 2003 and 2004) re-analyzed the stretching problem discussed earlier by Elbashbeshy (1998) including variable viscosity, internal heat generation, suction or injection and porous medium. Micropolar fluids are referred to those fluids that contain micro-constituents that can undergo rotation which affect the hydrodynamics of the flow. In this context, they can be distantly non-Newtonian in nature. The basic continuum theory for this class of fluids was originally formulated by Eringen (1966). The theory of thermo micropolar fluids has been developed by Eringen (1972) by extending the theory of micropolar fluids (1966)]. The Study of micropolar fluid mechanics has received the attention of several a research workers. Review of this study was provided by Ishak et al. (2007, 2008), Nazar et al. (2008) and Elbashbeshy et al. (2011). In the presented study, the effects of thermal radiation, magnetic field and internal heat generation on heat transfer in a micropolar fluid

*Corresponding Author E-mail: essamscience80@yahoo.com

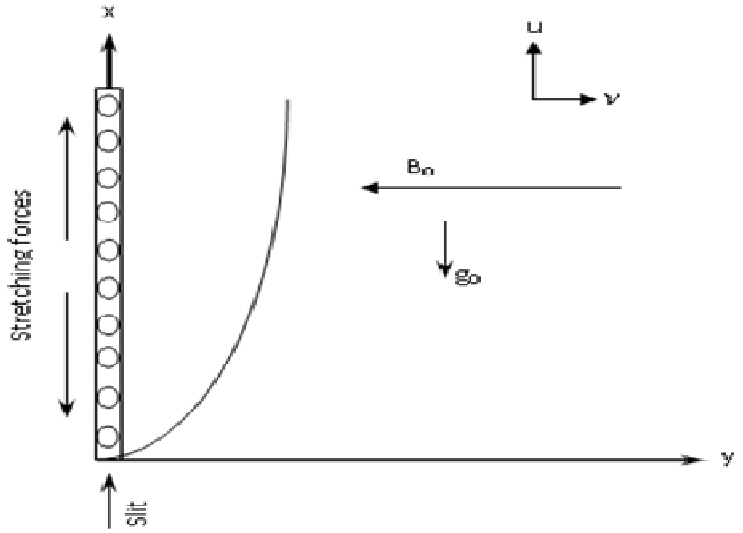

Figure 1. Physical model and coordinate system.

along a vertical porous stretching surface with variable viscosity has been investigated.

Mathematical Formulation

Consider steady, laminar, two-dimensional and magneto hydrodynamics boundary layer flow of a micropolar fluid along a vertical porous stretching surface in the presence of heat generation or absorption, thermal radiation, variable viscosity and viscous dissipation effect. The fluid is assumed to be viscous and has constant properties except the viscosity. Two–equal and opposite forces are introduced along x-axis so that the surface is stretched keeping the origin fixed and y-axis is perpendicular to it. A uniform magnetic field B_o is imposed along the y-axis and the magnetic Reynolds is assumed to be small so that the induced magnetic field is neglected. No electric field is assumed to exist and the hall effect of magnetohydrodynamics is neglected. The fluid is considered to be gray; absorbing–emitting radiation but non-scattering medium and Roseland approximation is used to describe the radiative heat flux in the energy equation. The radiative heat flux in the x-direction is considered negligible in comparison to the y-direction.

The governing boundary layer equations may be written as follows.(Figure 1)

$$\frac{\partial u}{\partial x}+\frac{\partial v}{\partial y}=0 \tag{1}$$

$$u\frac{\partial u}{\partial x}+v\frac{\partial u}{\partial y}=\frac{1}{\rho_\infty}\frac{\partial}{\partial y}((\mu+S)\frac{\partial u}{\partial y})+\frac{S}{\rho_\infty}\frac{\partial N}{\partial y}+g\beta(T-T_\infty)-\frac{\sigma^* B_0^2}{\rho_\infty}u \tag{2}$$

$$u\frac{\partial N}{\partial x}+v\frac{\partial N}{\partial y}=\frac{\upsilon_s}{\rho_\infty j}\frac{\partial^2 N}{\partial y^2}-\frac{S}{\rho_\infty j}(2N+\frac{\partial u}{\partial y}) \tag{3}$$

$$u\frac{\partial T}{\partial x}+v\frac{\partial T}{\partial y}=\frac{k}{\rho_\infty c_p}\frac{\partial^2 T}{\partial y^2}+\frac{Q_0}{\rho_\infty c_p}(T-T_\infty)+\frac{\mu}{\rho_\infty c_p}(\frac{\partial u}{\partial y})^2-\frac{1}{\rho_\infty c_p}\frac{\partial q_r}{\partial y} \tag{4}$$

Where u, v are the velocity component along x, y directions respectively, ρ_∞ is the density of the ambient fluid, μ is the coefficient of dynamic viscosity, S is the coefficient vortex viscosity, N is the angular velocity or micro rotation, g is the acceleration due to gravity , β is the volumetric coefficient of thermal expansion, υ_s is the spin-gradient viscosity , σ^* is the electrical conductivity of the fluid, B_o is the magnetic induction, j is the micro-inertia per unit mass, T is the temperature of the fluid within boundary layer, T_∞ is the temperature of the ambient fluid, k is the thermal conductivity, c_p is the specific heat due to constant pressure, Q_o is the heat generation or absorption coefficient and q_r is the radiative heat flux.

The boundary conditions for this problem can be written as

$$y=0: u=cx^m,\ v=v_0(x),\ N=-n\frac{\partial u}{\partial y},\ T=T_w \tag{5}$$

$$y\to\infty: u=0,\ N=0,\ T=T_\infty.$$

Where c is stretching coefficient, m is the stretching index, T_w is the temperature at the surface and n is the micro rotation parameter ($o \le n \le 1$). It should be mentioned that the case n = 0 . we obtain N = 0 which represents a no – spin condition i.e. the microelements in concentrated particle flow close to the wall are not able

to rotate (called strong concentration). The case n= 0.5 represents vanishing of the anti-symmetric part of the stress tensor (called weak concentration). The case n=1 is representative of turbulent boundary layer. The positive and negative values of v_o indicate injection and suction respectively, while v_o= 0 correspond to an impermeable surface.

By using Roseland approximation q_r take the form

$$q_r = -\frac{4\sigma_1}{3k_1}\frac{\partial T^4}{\partial y} \tag{6}$$

where σ_1 is the Stefan-Boltzmann constant and k_1 is the mean absorption coefficient. We assume that the temperature difference within the flow are sufficiently small such that T^4 may be expressed as a linear function of temperature. This is accomplished by

$$T^4 \cong T_\infty^4 + (T - T_\infty)4T_\infty^3 + \ldots\ldots = 4T_\infty^3 T - 3T_\infty^4 \tag{7}$$

By using Eqs. (6) and (7) in (4) gives

$$u\frac{\partial T}{\partial x} + v\frac{\partial T}{\partial y} = \frac{k}{\rho_\infty c_p}\frac{\partial^2 T}{\partial y^2} + \frac{Q_0}{\rho_\infty c_p}(T - T_\infty) + \frac{\mu}{\rho_\infty c_p}\left(\frac{\partial u}{\partial y}\right)^2 + \frac{16\sigma_1 T_\infty^3}{3k_1\rho_\infty c_p}\frac{\partial^2 T}{\partial y^2} \tag{8}$$

The following non-dimensional variables are introduced in order to obtain the non-dimensional equations:

$$\eta = y\sqrt{\frac{c}{\nu_\infty}}x^{\frac{m-1}{2}}, \psi(x, y) = \sqrt{c\nu_\infty}x^{\frac{m+1}{2}} f(\eta),$$
$$N = \sqrt{\frac{c^3}{\nu_\infty}}x^{\frac{3m-1}{2}}\phi(\eta), \theta = \frac{T - T_\infty}{T_w - T_\infty}, T_w - T_\infty = Ax^p \tag{9}$$

Where ψ is the stream function defined as $u = \frac{\partial \psi}{\partial y}$ and $v = -\frac{\partial \psi}{\partial x}$, which identically satisfy (1). We have from equation (9), that

$$u = cx^m f'(\eta), \quad v = -\sqrt{c\nu_\infty}x^{\frac{m-1}{2}}\left[\frac{m+1}{2}f(\eta) + \frac{m-1}{2}\eta f'(\eta)\right] \tag{10}$$

Where η is the similarity variable, f is the dimensionless stream function, ϕ is the dimensionless micro rotation, θ is the dimensionless temperature, A is constant, p is the temperature index and prime denotes differentiation with respect to η.

For a viscous fluid, Ling and Dybb (1987) suggest a viscosity dependence on temperature T of the form

$$\mu = \frac{\mu_\infty}{1 + \gamma_1(T - T_\infty)} \tag{11}$$

Where γ_1 is the thermal property of the fluid and μ_∞ is the coefficient of dynamic viscosity of the ambient fluid Equation (11) can be written as (7)

$$\frac{1}{\mu} = \alpha(T - T_r) \tag{12}$$

Where

$$\alpha = \frac{\gamma_1}{\mu_\infty} \quad \text{and} \quad T_r = T_\infty - \frac{1}{\gamma_1} \tag{13}$$

In the above relation (13) both α and T_r are constant and their values depend on the reference state and γ_1. In general, $\alpha > 0$ for liquids and $\alpha < 0$ for gases.

The dimensionless temperature $\theta(\eta)$ can be written as

$$\theta(\eta) = \frac{T - T_r}{T_w - T_\infty} + \theta_r, \text{ where}$$

$$\theta_r = \frac{T_r - T_\infty}{T_w - T_\infty} = -\frac{1}{\gamma_1(T_w - T_\infty)} = \text{constant} \tag{14}$$

and its value is determined by the viscosity/characteristics of the fluid under consideration and temperature difference $\Delta T = T_w - T_\infty$. Substituting equation (14) into (11), we obtain

$$\mu = \mu_\infty\left(\frac{\theta_r}{\theta_r - \theta}\right) \tag{15}$$

Now substituting Eqs. (9), (10) and (15) into Eqs. (2), (3) and (8) we obtain the following non-dimensional equations.

$$\left(K + \frac{\theta_r}{\theta_r - \theta}\right)f''' + \frac{m+1}{2}ff'' - mf'^2 + \frac{\theta_r}{(\theta_r - \theta)^2}f''\theta + K\phi - Mf' + \gamma\theta = 0 \tag{16}$$

$$\left(\frac{\theta_r}{\theta_r - \theta} + \frac{K}{2}\right)\xi\phi'' - \xi\left(\frac{3m-1}{2}\phi f' - \frac{m+1}{2}f\phi'\right) - K(2\phi + f'') = 0 \tag{17}$$

$$(1+R)\theta'' + \Pr_\infty\left[\left(\frac{m+1}{2}f\theta' - pf'\theta\right) + Q\theta + \frac{\theta_r}{\theta_r - \theta}E_c f''^2\right] = 0. \tag{18}$$

Where $K = \frac{S}{\mu_\infty}$ is the vortex viscosity parameter, $M = \frac{\sigma^* B_0^2}{\rho_\infty c_p}x^{1-m}$ is the local magnetic field parameter, $\xi = \frac{jc}{\upsilon_\infty c_p}x^{m-1}$ is the local spin gradient viscosity parameter, $E_c = \frac{(cx^m)^2}{c_p(T_w - T_\infty)}x^{1-m}$ is the local Eckert number, $P_{r\infty} = \frac{c_p\mu_\infty}{k}$ is the ambient Prandtl number, $Q = \frac{Q_0}{\rho_\infty c_p c}x^{1-m}$ is the local heat source (or

sink) parameter, $\gamma = \frac{Gr_x}{\mathrm{Re}_x}$ is the Richardson parameter, $Gr_x = \frac{g\beta(T_w - T_\infty)x^3}{\upsilon_\infty^2}$ is the local Grashof number, $\mathrm{Re}_x = \frac{cx^{m+1}}{\upsilon_\infty}$ is the local Reynolds number and $R = \frac{16\sigma T_\infty^3}{3k_1 k}$ is the thermal radiation parameter.

The assumption of Prandtl number inside the boundary layer may produce unrealistic results. Therefore, the Prandlt number related to the variable viscosity is defined by

$$\mathrm{P}_{rv} = \frac{\mu c_p}{k} = (\frac{\theta_r}{\theta_r - \theta})\frac{\mu_\infty c_p}{k} = (\frac{\theta_r}{\theta_r - \theta})P_{r\infty} \quad (19)$$

Substituting eq. (19) into (18), we obtain

$$(1+R)\theta'' + \mathrm{Pr}_v[\frac{\theta_r - \theta}{\theta_r}(\frac{m+1}{2}f\theta' - pf'\theta + Q\theta) + E_c f''^2] = 0. \quad (20)$$

In the case $\theta_r \to \infty$, $\eta = 0$ the variable Prandtl number $\mathrm{Pr}_v = \mathrm{Pr}_\infty$ and equation (20) reduces to (18). In the case $\eta \to \infty$, i.e. $\theta = 0$, the variable Prandtl number $\mathrm{Pr}_v = \mathrm{Pr}_\infty$. Equation (20) is corrected non-dimensional from of the energy equation for modeling thermal boundary layer flows with variable viscosity.

The dimensionless form of the boundary conditions becomes

$$\eta = 0 : f = f_w,\ f' = 1,\ \phi = -nf'',\ \theta = 1$$
$$\eta \to \infty : f' = 0,\ \phi = 0,\ \theta = 0. \quad (21)$$

Where $f_w = \pm \frac{v_0(x)}{\sqrt{c\upsilon_\infty}\ \frac{m+1}{2}x^{\frac{m-1}{2}}}$ is the suction(injection) parameter

Nusselt number

The local heat flux may be written as

$$q_w = k(\frac{\partial T}{\partial y})_{y=0} + q_r\big|_{y=0}$$

The local Nusselt number may be written as

$$Nu_x = -\frac{q_w x}{k(T_w - T_\infty)}$$

$$\frac{Nu_x}{\sqrt{\mathrm{Re}_x}} = -(1+R)\theta'(0)$$

Numerical Solutions

The Equations (16-18) can be converted to a system of differential equations of first order, by using

$y_1 = f,\ y_2 = f',\ y_3 = f'',\ y_4 = \phi,\ y_5 = \phi',\ y_6 = \theta,\ y_7 = \theta',$

$y_1' = y_2,$

$y_2' = y_3,$

$$(K + \frac{\theta_r}{\theta_r - y_6})y_3' = my_2^2 - \frac{m+1}{2}y_1 y_3 + My_2 - \gamma\theta + \frac{\theta_r}{(\theta_r - y_6)^2}y_7 y_3 - Ky_5,$$

$y_4' = y_5,$

$$(\frac{\theta_r}{\theta_r - y_6} + \frac{K}{2})\xi y_5' = \xi(\frac{3m-1}{2}y_2 y_4 - \frac{m+1}{2}y_1 y_5) + K(2y_4 + y_3),$$

$y_6' = y_7,$

$$(1+R)y_7' = -P_w(1 - \frac{y_6}{\theta_r})[\frac{m+1}{2}y_1 y_7 - py_2 y_6 - Qy_6] - P_w E_c y_3^2. \quad (22)$$

Subjected to the initial conditions

$$y_1(0) = f_w,\ y_2(0) = 1,\ y_3(0) = a,\ y_4(0) = -ny_3(0),\ y_5(0) = b,\ y_6(0) = 1,\ y_7(0) = c. \quad (23)$$

Where a, b and c are unknown to be determined as a part of the numerical solution. Using mathematica, a function (F) has been defined such that F [a, b, c]:=NDSolve [system (22),(23)], The value of *a*, b and c are determined upon solving the equations, $y_2(\eta_{\max}) = 0,\ y_4(\eta_{\max}) = 0$ and $y_6(\eta_{\max}) = 0$ to get the solution, NDSolve first searches for initial conditions that satisfy the equations, using a combination of Solve and a procedure much like Find Root. Once a, b and c are determined the system (22) and (23) is closed, it can be solved numerically using the ND Solve function.

RESULTS AND DISCUSSION

The set of non-linear ordinary differential equations (16), (17) and (20), satisfying the boundary conditions (21) have been solved numerically using the mathematica method for several values of the involved parameters , namely the vortex viscosity parameter (K), local magnetic field parameter (M) , local spin gradient viscosity parameter (ξ) , Eckert number (Ec), local heat source (or sink) parameter (Q), Richardson parameter (γ), Temperature index (p), Stretching index (m) and variable Prandtl number (Pr_v). It is found that the values of the local Nusselt number ($Nu_x / \sqrt{\mathrm{Re}_x}$) compare with the results reported by Ali (19) and Rahman et al (20) as shown in Table 1. These comparisons show excellent agreement between the results.

Table 1. Comparisons of $\theta'(0)$ to previously published data at $Pr_\infty = 0.7$, K =0, R= 0, ξ = 0, γ = 0, M = 0, Q = 0, Ec = 0, m = 0 and p = 0 for different values of θr .

θr	Ali (Ali, 2006)	Rahman (Rahman et al, 2009)	Present results
–8.0	–0.3432339	–0.3436723	-0.3432256
–0.1	–0.1652394	–0.1661476	-0.1660486
–0.01	–0.0561845	–0.0764055	-0.0544607
8.0	–0.3555822	–0.3560031	-0.3579886

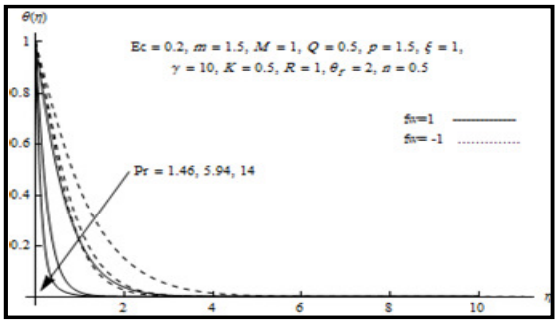

Figure 2. Temperature profiles $\theta(\eta)$ for some values of Pr

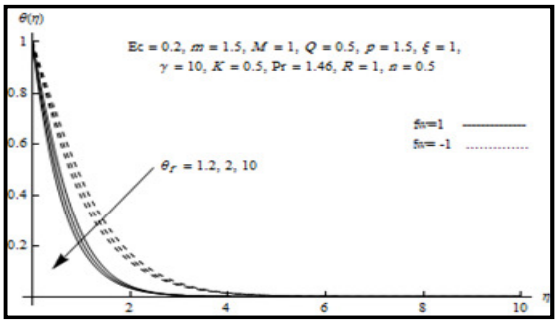

Figure 3. Temperature profiles $\theta(\eta)$ for some values of θ_r

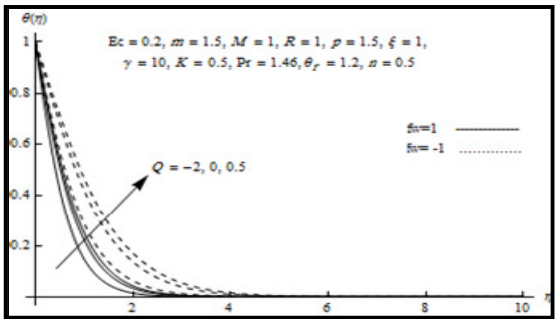

Figure 4. Temperature profiles $\theta(\eta)$ for some values of Q

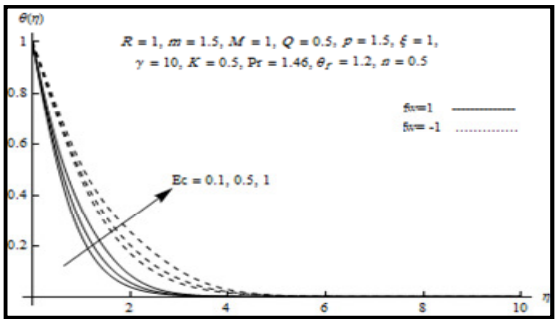

Figure 5. Temperature profiles $\theta(\eta)$ for some values of E_c

Figure (2) represents , the temperature profiles for different values of variable Prandtl number Pr_v .It seen that the effect of variable Prandtl number Pr_v is to decrease temperature throughout the boundary layer ,which results in decrease of the thermal boundary layer thickness with the increase of values of Pr_v. The increase of variable Prandtl number means slow rate of thermal diffusion. It is also observe that for a fixed value of Pr_v, the temperature corresponding to the case of fluid suction is lower compared to the case of fluid injection. That is, the thickness of the thermal boundary layer is higher for fluid injection than for fluid suction.

Figure (3) represents the temperature profiles for different values of fluid viscosity parameter θr. The figure indicates that the boundary layer thickness decreases with the increase of values of fluid viscosity θr for both cases of fluid suction and injection. It is seen that for fluid suction, the temperature decreases very rapidly with η. Whereas in the case of fluid injection, the temperature decreases very steadily. Further it is observed that the decrease in the temperature with θr is not very remarkable near the boundary in this case. This effect is much noticeable little away from stretching surface.

Figure (4) illustrates the dimensionless temperature profiles for different values of the heat generation (or absorption) parameter Q. It is observed from this figure the boundary layer generates the energy, which causes the temperature profiles to increase with increasing the heat generation for both cases of fluid suction and injection. But the opposite effect is observed for the case of heat absorption. The thickness of the thermal boundary layer is high for fluid injection than for fluid suction for both cases of heat generation or absorption.

Figure (5) represents the temperature profiles for

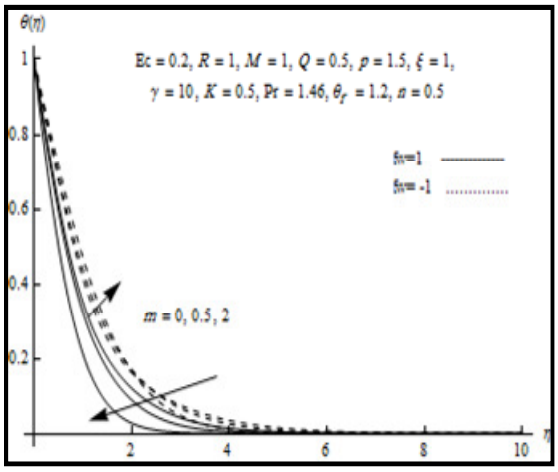

Figure 6. Temperature profiles $\theta(\eta)$ for some values of m

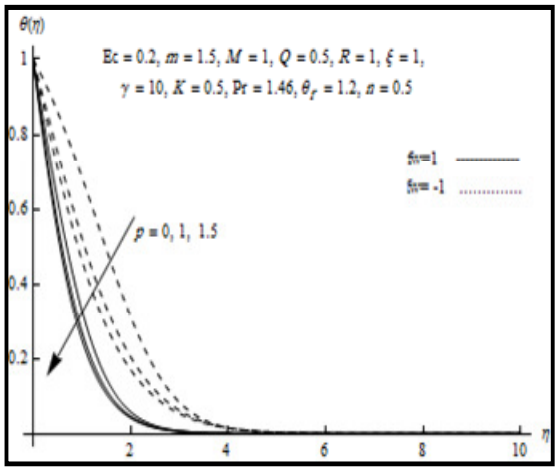

Figure 7. Temperature profiles $\theta(\eta)$ for some values of p

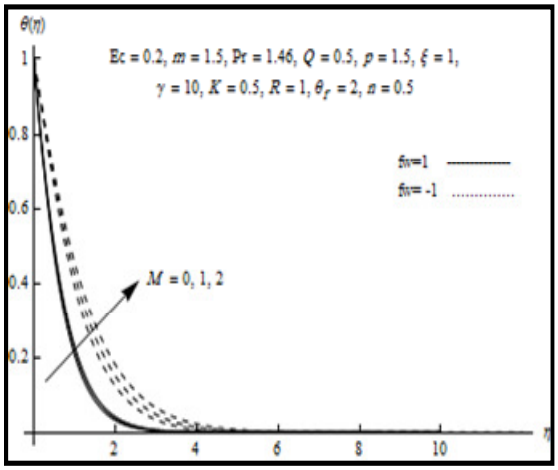

Figure 8. Temperature profiles $\theta(\eta)$ for some values of M

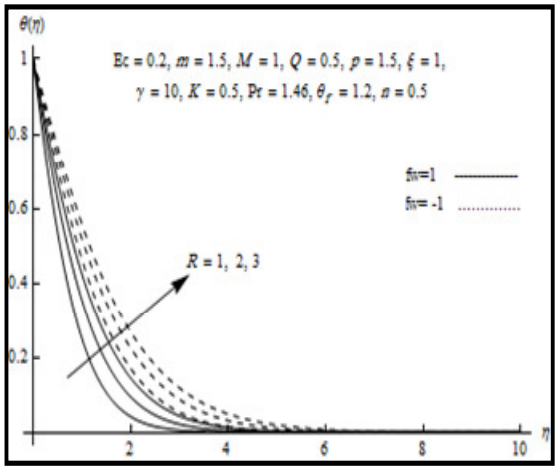

Figure 9. Temperature profiles $\theta(\eta)$ for some values of R

various values of Eckert number Ec. This figure indicates that the temperature profiles have an increasing effect for increasing values of Ec. therefore, increasing the Eckert number Ec broadens the thickness of the thermal boundary layer for both cases suction and injection .

Figure (6) explains the effect of stretching index m on the temperature profiles. This figure indicates that the temperature profiles decrease quite rapidly with an increase of m for the case fluid suction while the temperature profiles increase for the case fluid injection.

Figure (7) represents the temperature profiles for various values of the temperature index p. From this figure we see that the temperature profiles decrease very rapidly in the case of fluid suction compared to the case of fluid injection with the increase of p.

Figure (8) represents the temperature profiles for various values of magnetic field parameter M.The presence of a magnetic field has a tendency to produce a drag-like force called the Lorentz force which acts in the opposite direction of the fluid motion. This causes the fluid temperature to increase as the magnetic field parameter M increases.

Figure (9) represents the temperature profiles for various values of the thermal radiation parameter R in the boundary layer. This figure indicates that the effect of thermal radiation is to enhance heat transfer because of the fact that thermal boundary layer thickness increase with increase in thermal radiation. Thus it is point out that the radiation should be minimized to have the cooling process at a faster rate.

Table 2. Results of the local Nusselt number $Nu_x / \sqrt{\mathrm{Re}_x}$ in case of f_w =1,-1 for different values of Richardson parameter γ and variable Prandtl number Pr_v at Ec =0.2, m=1.5, M=1, Q=0.5, p=1.5, ξ=1, K=0.5, R=1, n=0.5 and $\theta_r = 2$

Pr_v	1.46		5.94	
γ	f_w = 1	f_w = -1	f_w = 1	f_w = -1
2	2.126459	0.921387	6.523081	1.275471
4	2.297193	1.099709	6.666328	1.472371
6	2.414686	1.208343	6.724279	1.584499
8	2.500687	1.281266	6.901759	1.657344
10	2.564690	1.329710	6.918758	1.684404

Table 3. Results of the local Nusselt number $Nu_x / \sqrt{\mathrm{Re}_x}$ in case of f_w =1,-1 for different values of thermal radiation parameter R and Local heat source (or sink) parameter Q at Ec =0.2, m=1.5, M=1, γ=10, Pr_v =1.46, p=1.5, ξ=1, K=0.5, n=0.5 and $\theta_r = 2$

R	0.5		1	
Q	f_w = 1	f_w = -1	f_w = 1	f_w = -1
-2	4.206045	2.525405	2.648071	1.708477
-1	2.855495	1.597121	2.388218	1.451863
0	2.513991	1.259472	2.091386	1.160620
1	2.107175	0.860049	1.737748	0.817026
2	1.587357	0.376250	1.285922	0.399245

Table (2) show the local Nusselt number $Nu_x / \sqrt{\mathrm{Re}_x}$ for different values of Richardson parameter γ and variable Prandtl number Pr_v. This table show that for a fixed value of Pr_v, the local Nusselt number $Nu_x / \sqrt{\mathrm{Re}_x}$ increases with the increase of the Richardson parameter γ and variable Prandtl number Pr_v for both cases of fluid suction and injection. Thus, applying suction/ injection one can control the heat transfer from heated surface to the fluid.

Table (3) show the local Nusselt number $Nu_x / \sqrt{\mathrm{Re}_x}$ for different values of heat generation (or absorption) parameter Q and thermal radiation R. From this table we show that for a fixed value of thermal radiation parameter R the local rate of heat transfer from the surface to the fluid decrease with the increase of the heat generation parameter for both cases of fluid suction and injection. This is due to the fact that as heat is generated, the thermal state of the surrounding fluid increase, as a consequence, the rates of heat transfer from the surface to the fluid decreases. Table (3) also show that for a fixed value of heat generation or absorption parameter the values of $Nu_x / \sqrt{\mathrm{Re}_x}$ decrease with the increase of the thermal radiation parameter R for both fluid suction and injection. On the other hand, values of $Nu_x / \sqrt{\mathrm{Re}_x}$ decrease very rapidly with the increase of the thermal radiation parameter for the case suction compared to that of fluid injection.

Table (4) shows the local Nusselt number $Nu_x / \sqrt{\mathrm{Re}_x}$ for different values of magnetic field parameter M and viscosity parameter θr. This table show that for a fixed value of θr, the local Nusselt number $Nu_x / \sqrt{\mathrm{Re}_x}$ decreases with increase of the magnetic field parameter M for both cases of fluid suction and injection. From here we found that for a fixed value of M, the local Nusselt number $Nu_x / \sqrt{\mathrm{Re}_x}$ increases with the increase of variable viscosity θr.

Table 4. Results of the local Nusselt number $Nu_x / \sqrt{\mathrm{Re}_x}$ in case of f_w =1,-1 for different values of magnetic field parameter M and Variable viscosity parameter θr at Ec =0.2, R=1, Q=0.5, m=1.5, γ=10, Pr_v =1.46, p=1.5, ξ=1, K=0.5, and n=0.5

θr	2		5	
M	**f_w = 1**	**f_w = -1**	**f_w = 1**	**f_w = -1**
0	2.635628	1.381881	3.037265	1.479986
0.5	2.600075	1.356747	2.997939	1.456576
1	2.564690	1.329710	2.958341	1.430489
1.5	2.529706	1.299828	2.918862	1.400753
2	2.495270	1.272607	2.897410	1.372954

Table 5. Results of the local Nusselt number $Nu_x / \sqrt{\mathrm{Re}_x}$ in case of f_w=1,-1 for different values of thermal radiation parameter R and Temperature index p at Ec =0.2, Q=0.5, m=1.5, γ=10, Pr_v=1.46, M=1, ξ=1, K=0.5, n=0.5 and $\theta_r = 2$

p	1		2	
R	**f_w = 1**	**f_w = -1**	**f_w = 1**	**f_w = -1**
0	1.901483	0.571333	2.144131	0.942772
1	2.347247	1.046684	2.764039	1.574413
2	2.712083	1.434293	3.243446	2.083120
3	3.031310	1.772078	3.661389	2.523179
4	3.319712	2.075794	4.037864	2.917297

Table (5) shows the local Nusselt number $Nu_x / \sqrt{\mathrm{Re}_x}$ for different values of thermal radiation parameter R and temperature index p for both cases of fluid suction and injection. From this table we can see that the values of $Nu_x / \sqrt{\mathrm{Re}_x}$ increase with the increase of temperature index p for fluid suction. The opposite trend is observed for the case of fluid injection.

CONCLUSION

In this paper, we have studied the problem of the boundary layer flow of a micropolar fluid and heat transfer on a vertical stretching surface with a variable viscosity and internal heat generation in the presence of magnetic field. The governing boundary layer equations were solved numerically .The development of the heat transfer rate at the surface, as well as the temperature has been illustrated in the tables and graphs. A discussion of the effects of the variable Prandtl number, Richardson parameter, Variable viscosity parameter, thermal radiation parameter , Magnetic field parameter, Local heat source (or sink) parameter and Temperature index on the heat transfer rate at the surface in the case $n = 0.5,\ f_w = 1, -1$ has been obtained.

From the present investigation, the following conclusions may be concluded.

The local Nusselt number decreases with the increase of the heat generation parameter, thermal radiation parameter, magnetic field parameter and increases with the increase of the heat absorption parameter, variable Prandtl number, variable viscosity parameter, temperature index parameter and Richardson parameter.

REFERENCES

Ali ME (1995). on thermal boundary layer on a power law stretched surface with suction or injection. Int. J. Heat Mass Flow. 16:280-290.

Ali ME (2006). The effect of variable viscosity on mixed convection heat transfer along a vertical moving surface. Int.J. Thermal Sci. 45:60-69.

Banks WHH (1983). Similarity Solution of the boundary layer equation for a stretching wall. J. Mech. Theory Appl. 2:375-392.

Crane LJ (1970). Flow past a stretching plane. Z. Amgew Math. Phys. 21:645-647.

Elbashbeshy EMA, Aldawody DA (2011). Heat transfer over an unsteady stretching surface in a micropolar fluid in the presence of magnetic field and thermal radiation. Can. J. Phys. 89:259-298.
Elbashbeshy EMA (1998). Heat transfer over a stretching surface with variable heat flux. J.Phys.D:Appl. Phys. 31:1951-1955.
Elbashbeshy EMA, Bazid MAA (2000). Heat transfer over a continuous moving plate embedded in a non-Darcian porous medium. Int. J. Heat Mass Transfer. 43:3087-3092.
Elbashbeshy EMA, Bazid MAA (2000). The effect of temperature dependent viscosity on heat transfer over continuous moving surface. J. Phys.D. Appl.Phys. 33:2716-2721.
Elbashbeshy EMA, Bazid MAA (2003). Heat transfer over a stretching surface with internal heat generation. Con.J.Phys. 81(4):699-703.
Elbashbeshy EMA, Bazid MAA (2003). Heat transfer over an unsteady stretching surface with internal heat generation. Appl. Math. Comput. 138(3):239-245.
Elbashbeshy EMA, Bazid MAA (2004). Heat transfer in a porous medium over a stretching surface with internal heat generation and suction or injection. Appl. Math. Comput. 158(3):799-807.
Eringen AC (1966). Theory of micropolar fluids. J. Math Mech.16:1-18.
Eringen AC (1972). Theory of thermo micro fluids. J. Math. Analysis Applications. 38:480-496.
Ishak A, Nazar R, Pop I (2007). MHD stagnation point flow towards a stretching vertical sheet in a micropolar fluid, Magnetohydro dynamics. 43(1):83-79.
Ishak A, Nazar R, Pop I (2008). Heat transfer over a stretching surface with variable surface heat flux in micropolar fluids. Phys. Lett. 372:559-561.
Ishak A, Nazar R, Pop I (2008). Unsteady boundary layer flow over a stretching sheet in micropolar fluid. Int. J. Math, Phys and Eng. Sci. 2(3):161-165.
Link JX, Dybbs A (1987). Forced convection over a flat plate submersed in a porous medium. ASME Paper 87WA/HT-23 New York.
Rahman MM, Samad ME, Alam MA (2009). Heat transfer in a micropolar fluid along a non-linear stretching sheet with a temperature-dependent viscosity and variable surface temperature. Int. J. Thermophys. 30:1649-1670.
Sakiadis BC (1961). Boundary layer behavior on continuous solid surfaces: I. Boundary layer equations for two dimensional and axisymmetric flow. AIChE J. 7(1):26-28.
Sakiadis BC (1961). Boundary layer behavior on continuous solid surfaces: II. Boundary layer equations on a continuous flat surface. AIChE. J. 7(1):221-225.